



## Transboundary Trajectory Patterns of PM<sub>2.5</sub> in The Lower Troposphere of Jakarta Region

Sifa Istiqomah<sup>1</sup>, I Putu Santikayasa<sup>1</sup>, Ana Turyanti<sup>1\*</sup>

<sup>1</sup> Department of Geophysics and Meteorology, IPB University, Bogor, Indonesia.

### ARTICLE INFO

#### Received

25 August 2025

#### Revised

01 December 2025

#### Accepted for Publication

03 December 2025

#### Published

30 December 2025

doi: [10.29244/j.agromet.39.2.107-119](https://doi.org/10.29244/j.agromet.39.2.107-119)

#### Correspondence:

Ana Turyanti  
Department of Geophysics and  
Meteorology, IPB University, Dramaga  
Campus, Bogor, Indonesia 16680.

Email: [ana@apps.ipb.ac.id](mailto:ana@apps.ipb.ac.id)

This is an open-access article  
distributed under the CC BY License.  
© 2020 The Authors. *Agromet*.

### ABSTRACT

PM<sub>2.5</sub> is a key indicator of air quality and poses serious environmental and health concern, especially in Jakarta where air quality frequently exceeds recommended standards. But researches mainly focus on surface-level pollutant, underscoring transboundary emission. This study aims to analyze the transboundary trajectory patterns of PM<sub>2.5</sub> pollutants, and to estimate the contribution of emissions to air quality in the Jakarta for 2024. Meteorological data and PM<sub>2.5</sub> concentrations from five air quality monitoring stations were analyzed during non-rainfall periods. Potential emission sources analysis was simulated using HYSPLIT Concentration Weighted Trajectory (CWT). Our results show PM<sub>2.5</sub> concentrations during the wet season were ~40% lower than dry season, with an average concentration of 27.11 µg/m<sup>3</sup> and were strongly influenced by monsoonal wind patterns in both seasons. During the west monsoon, pollutant transport was predominantly from the southwest to northeast, whereas during the east monsoon it shifted from the northwest to northeast. The trajectory patterns exhibited no substantial differences across all layers (15, 50, 100, and 200 m), although seasonal atmospheric stability influenced pollutant dispersion. In the wet season, PM<sub>2.5</sub> primarily originated from western regions of Jakarta, while in the dry season sources were predominantly from the east, which is consistent with prevailing monsoonal winds. Several monitoring stations also indicated potential contributions from North Jakarta due to curved airflow patterns. These findings highlight the dominant role of monsoonal wind in controlling PM<sub>2.5</sub> concentrations and transboundary transport in Jakarta within the lower troposphere.

### KEYWORDS

air quality, emission sources, HYSPLIT, monsoon, wind direction

## 1. INTRODUCTION

Air quality plays a critical role in human health and environment (Doherty et al., 2017; Almetwally et al., 2020). The exposure to air pollution beyond established standards can disrupt physiological systems and increase morbidity and mortality rates (Khaniabadi et al., 2019). Short-term exposure is associated with respiratory symptoms such as coughing and wheezing, whereas long-term exposure contributes to chronic asthma and pulmonary insufficiency (Manosalidis et al., 2020). Air pollution exposure during early life stages has been linked to perinatal disorders and an elevated

risk of chronic diseases later in adulthood (Hehua et al., 2017; Kravitz-Wirtz et al., 2018). Among various air pollutants, particulate matter (PM) is widely used as a key indicator of air quality (Beloconi and Vounatsou, 2021), particularly fine particulate matter (PM<sub>2.5</sub>), which has an aerodynamic diameter of less than 2.5 µm (Choi et al., 2024). Due to its small size, PM<sub>2.5</sub> can remain suspended in the atmosphere for extended periods, travel across administrative boundaries, and penetrate deeply into the respiratory system and bloodstream, posing severe health risks (Hao and Liu, 2016; Thangavel et al., 2022).

The atmospheric behavior of PM<sub>2.5</sub> is strongly influenced by emission characteristics, meteorological conditions, and the vertical structure of the atmosphere (Rawat et al., 2024). Major anthropogenic sources of PM<sub>2.5</sub> include residential heating, industrial combustion, and road transportation (Squizzato et al., 2017). The height of emission sources plays a crucial role in determining pollutant dispersion pathways. Emissions released below the planetary boundary layer (PBL) tend to remain confined near the surface and disperse through local advection, whereas emissions released above the PBL can be transported over long distances within the free troposphere, contributing to regional and transboundary air pollution (Đorđević and Šolević, 2008). In addition, atmospheric phenomena such as temperature inversions can suppress vertical mixing and exacerbate pollutant accumulation near the surface (Wu et al., 2014). Surface meteorological factors-including air temperature, relative humidity, wind speed and direction, and rainfall-also significantly influence pollutant formation, dispersion, and removal processes (Kayes et al., 2019; Ni et al., 2023).

Studies have demonstrated that PM<sub>2.5</sub> sources often originate beyond local administrative boundaries and vary with altitude and season. For instance, study in Shenyang, China analyzed emission sources at multiple atmospheric heights, revealing that pollution was dominated by short- and medium-range transport from surrounding regions (Ma et al., 2020). Similarly, other study reported that PM<sub>2.5</sub> concentrations in Thimphu, Bhutan, were largely influenced by trans-boundary emissions from neighboring countries (Sharma et al., 2022). Seasonal variability in emission source regions has also been observed, with studies indicating distinct source contributions between warm and cold seasons (Ma et al., 2022). These findings highlight that PM<sub>2.5</sub> pollution in urban areas is not solely driven by local emissions but is strongly affected by regional-scale atmospheric trans-port processes.

However, studies on PM<sub>2.5</sub> transport in the DKI Jakarta region remain limited. Existing research using the HYSPLIT Concentration Weighted Trajectory (CWT) model primarily focuses on surface-level transport or specific extreme events, such as forest fires, making it difficult to quantitatively assess elevated transport contributions from higher atmospheric layers. Moreover, limited studies have explicitly distinguished PM<sub>2.5</sub> transport during non-rainfall periods across wet and dry seasons, even though rainfall plays a key role in pollutant removal. To address these gaps, this study applies the HYSPLIT-CWT model to analyze PM<sub>2.5</sub> transport trajectories at multiple heights (15, 50, 100, and 200 m above ground level) during non-rainfall periods in both seasons. The objectives of this study are

to characterize transboundary PM<sub>2.5</sub> transport patterns and to estimate the contribution of emission sources at different altitudes to air quality of Jakarta region in 2024.

## 2. MATERIALS AND METHODS

### 2.1 Study Area

This study area covers DKI Jakarta, with five sub region (Figure 1). The focused area is on DKI Jakarta-capital city of Indonesia -at five DKI Jakarta Ambient Air Quality Monitoring Stations (SPKUA) named DKI1-DKI5 (Table 1). This area located on low-lands with a slope gradient of 0-3% and average elevation of 7 meters above sea level. The study area has monsoon rainfall pattern with only one peak during wet season. The dry season occurred in December-March with average rainfall >150 mm/month, while the wet season in June-September has <100 mm/month rainfall (Maheng et al., 2023).

### 2.2 Tools and Data Collections

We performed our analysis using R, HYSPLIT Concentration Weighted Trajectory (CWT), Meteo-infomap, Java Runtime Environment (JRE), Filezilla, and ArcGIS. The primary materials in this study utilized hourly meteorology (wind speed, wind direction, and rainfall) and PM<sub>2.5</sub> concentration data from air quality monitoring stations by Environmental Agency of DKI Jakarta. We also used 3-hourly Global Data Assimilation System (GDAS1) from National Oceanic and Atmospheric Administration (NOAA) as model input to HYSPLIT. The data period analyzed in this study spans two separate periods: January to February and July to September for representing wet and dry seasons during 2024. The pollution data analysis is considered during non-rainfall period, defined as a day with < 1 mm of rainfall in both seasons.

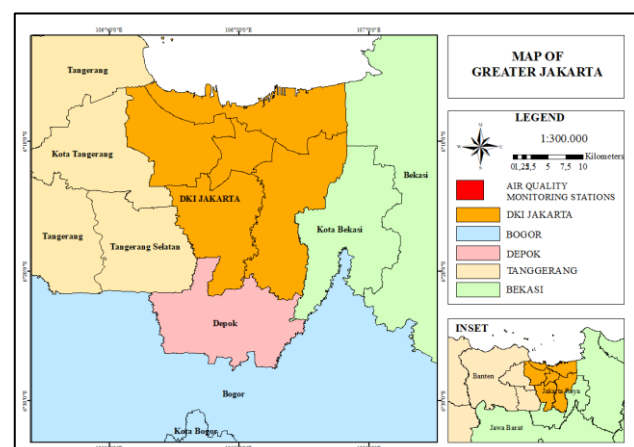


**Figure 1** Map of the study area (red boxes represents air quality monitoring stations)

**Table 1** Locations of the Jakarta Ambient Air Quality Monitoring Stations

| No | Station Name | Location                    | Land-use        | Coordinates |          |
|----|--------------|-----------------------------|-----------------|-------------|----------|
|    |              |                             |                 | Longitude   | Latitude |
| 1  | DKI1         | Bundaran HI-Central Jakarta | roadside        | 106.824     | -6.195   |
| 2  | DKI2         | Kelapa Gading-North Jakarta | commercial area | 106.911     | -6.155   |
| 3  | DKI3         | Jagakarsa-South Jakarta     | settlement      | 106.804     | -6.357   |
| 4  | DKI4         | Lubang Buaya-East Jakarta   | mixture         | 106.910     | -6.2889  |
| 5  | DKI5         | Kebo Jeruk-West Jakarta     | settlement      | 106.753     | -6.207   |

### 2.3 Determination of Non-rainfall Period

The PM<sub>2.5</sub> concentration analysis was conducted during non-rainfall periods (rainfall < 1 mm/day), due to potential rainfall effect on PM<sub>2.5</sub> reduction (Fujino and Miyamoto, 2022). The data of non-rainfall periods in DKI Jakarta in 2024 for dry and wet season which represented by January and February, then July to September, respectively (Table A1). In this study, a period is categorized as non-rainfall if there are at least 3 consecutive days without rain in a week. The determination of three consecutive days is based on the Consecutive Dry Days (CDD) index, which indicates the occurrence of consecutive days without rain or with less than 1 mm of rain. January and February are the months with the least numbers of data on non-rainfall, while August is the month with the most data for non-rainfall period in DKI1-DKI5 regions which represents both the peak period for each season. The peak of the wet season and dry season are influenced by monsoon winds, so the direction of the wind will affect the pattern of air masses entering the DKI Jakarta region and may carry pollutants within them.

### 2.4 Data Analysis

#### 2.4.1 PM<sub>2.5</sub> Concentration Analysis

The PM<sub>2.5</sub> concentration analysis from 5 Ambient Air Quality Monitoring Stations (SPKUA) in DKI Jakarta was conducted during non-rainfall period in dry and wet seasons. The measured pollutant concentrations originated from emission sources which fluctuations were not affected by rainfall presumably. The daily average PM<sub>2.5</sub> concentration was obtained using the arithmetic mean method (Eq. 1).

$$\mu = \frac{1}{N} \sum_{i=1}^N x_i \quad (1)$$

N is the total number of observations in a dataset, and x<sub>1</sub>, x<sub>2</sub>, ..., x<sub>n</sub> are individual observations. The average of all this data is constant and is a non-random variable, so that if different samples are taken from the same data, the same average value will always be obtained. The results of the daily average PM<sub>2.5</sub> concentration are used to analyze the estimated contribution of PM<sub>2.5</sub> emission sources during non-rainfall period using HYSPLIT CWT.

#### 2.4.2 Local Potential Emission Sources Analysis

The analysis of local potential emission sources in DKI Jakarta in 2024 was conducted using analysis of wind direction and wind speed data at each SPKUA. We use the monsoon period for separate dry (east monsoon wind) and wet season (west monsoon wind) which all months out of these period categorized as transitional months (Suhery et al., 2023). DKI Jakarta experiences the dominance of the west monsoon from December to March and the east monsoon from June to September. We performed the analysis using R package "openair" which generates polar plots. This package calculated back trajectories, commonly used in air pollution analysis. Additionally, the polar plots show pollutant concentrations based on wind speed and direction as a continuous surface as the representative between wind speed, direction and pollutant dispersion in polar coordinates (Carslaw and Beevers, 2013).

#### 2.4.3 Inter-regional Potential Emission Sources Analysis

Inter-regional emission source potential analysis was conducted using Hybrid Single-Particle Lagrangian Integrated Trajectory Concentration Weighted Trajectory (HYSPLIT CWT) to identify areas contributing to PM<sub>2.5</sub> concentrations in DKI Jakarta. HYSPLIT played a role in calculating backward trajectories of air mass using TrajStat software which contained in MeteoInfo. We used NOAA grid meteo-logical data from the Global Data Assimilation System (GDAS1) with 23 vertical levels from 1000 hPa to 20 hPa and a horizontal resolution of 1 latitude and 1 longitude used in the global HYSPLIT domain, as well as PM2.5 of the study areas used to identify contributions from air pollutant sources (Yin et al., 2021).

Backward trajectory simulations were conducted at several heights, including 15, 50, 100, and 200 meters above ground level (magl) selected to the possibility of emission sources from industrial chimneys at certain heights and their impact on air quality in Jakarta. The total runtime for each backward trajectory was 24 hours, with air masses appearing at 1-hour intervals. The determination of backward trajectories over 24 hours shows air trajectories closer to the surface, where most PM<sub>2.5</sub> pollutants are emitted, thereby more accurately indicating the direction of PM<sub>2.5</sub> pollutant sources

(Su et al., 2015). We divided 2 clustering of air mass flow based on the regions traversed by the trajectories. According to Li et al. (2017), airflow clustering is a multi-variate statistical analysis technique used to determine trajectories based on the similarity of spatial distribution characteristics. In HYSPLIT CWT, the first step is to calculate the concentration weights of the trajectories, then obtain the weighted concentrations of the grid. The calculation of concentration weights from the trajectories is based on the research by Yin et al. (2021). The calculation formula for the HYSPLIT CWT method in (Eq. 2).

$$CWT_{ij} = \frac{\sum_{k=1}^N C_k \tau_{ijk}}{\sum_{k=1}^N \tau_{ijk}} \quad (2)$$

Which  $CWT_{ij}$  is the average weight concentration of grid  $ij$ ,  $N$  is the total number of trajectories,  $k$  is the trajectory,  $C_k$  is the  $PM_{2.5}$  concentration on trajectory  $k$  when passing through grid  $ij$ , which can be calculated using the HYSPLIT model, and  $\tau_{ijk}$  is the duration of trajectory  $k$  in grid  $ij$ . The CWT method introduces significant uncertainty, so weight coefficients  $W_{ij}$  are needed to reduce this uncertainty (Eq. 3).

$$WCWT_{ij} = W_{ij} \times CWT_{ij} \quad (3)$$

### 3. RESULTS AND DISCUSSION

#### 3.1 Rainfall Characteristics

The climatic period of DKI Jakarta showed distinct pattern for each month throughout the year 2024, observed by monthly rainfall data (Figure 2). DKI Jakarta has two main seasons, including wet period in October to March and dry period from April to September. Our rainfall analysis showed the same pattern of dry and wet season started from May-October and November-April, respectively. The year 2024 was marked by moderate to strong El-Niño in July 2023 to June 2024 (Jiang et al., 2024), yielding relatively low rainfall amount with average monthly rainfall for all station is 80-90 mm. The dry season was indicated by low rainfall-below 100 mm, while the wet season has rainfall  $>100$  mm. The lowest monthly rainfall was observed during October with only 20 mm and the highest monthly rainfall occurred in February for all station. This also highlight the monsoon period for further emission sources analysis.

#### 3.2 $PM_{2.5}$ Concentration

$PM_{2.5}$  concentration values during the wet season (January-February) in the non-rainfall period were lower than the dry season (July-September) in the non-rainfall period (Figure 3). The average value represented by center line in the boxplot, wet season was 27.11 while in dry season was observed 44.87. The minimum

$PM_{2.5}$  concentration value during the wet season in the non-rainfall period was  $9.62 \mu g/m^3$ , while the maximum value was  $43.38 \mu g/m^3$ , with outliers of  $46.70 \mu g/m^3$  and  $49.22 \mu g/m^3$ . In the other hand, the minimum  $PM_{2.5}$  concentration during the dry season showed similar pattern in the non-rainfall period was  $23.15 \mu g/m^3$ , while the maximum was  $63.41 \mu g/m^3$ , with a lower outlier of  $15.23 \mu g/m^3$ . This highlight that seasonal monitoring of  $PM_{2.5}$  given different results in dry and wet season, which probably caused by other climatic factors on different season (Yang et al., 2017; Sanguineti et al., 2020). The  $PM_{2.5}$  concentrations during wet season undergo a washout process, facilitating wet deposition and dilution of pollutants in the atmosphere (Li et al., 2020). In this study,  $PM_{2.5}$  concentrations during the wet season were lower than during the dry season, even though the analysis was conducted under non-rainfall period. This may occurred by the increases of wind speed (Zhang et al., 2018) which is higher during the wet season, which is 0.67 m/s, compared to 0.56 m/s during the dry season.

#### 3.3 Local Wind Patterns and $PM_{2.5}$ Emissions

Local emission sources in the DKI1-DKI5 region are shown in a polar plot summary, with varying dominant wind directions (Table 2). According to Masiol et al. (2016), polar plots can reveal potential local emission sources. A summary of local emission sources from the polar plot, including dominant wind direction, wind speed, and  $PM_{2.5}$  concentrations in the DKI1-DKI5 regions, is shown in Table 2. Based on the table, it is shown that each DKI1-DKI5 region contributes to emissions in its area, with the highest  $PM_{2.5}$  emissions during the wet season range from 10 to  $40 \mu g/m^3$  accompanied by winds blowing from the southwest to the northeast. The highest  $PM_{2.5}$  concentrations was observed during the dry season range from 30 to over  $50 \mu g/m^3$  driven by winds blowing from the northwest to the northeast. In general, local wind speeds during the west monsoon (wet season) are higher, ranging from 0.5 to 5 m/s, than local wind speeds during the east monsoon (dry season), which range from 0.5 to 4 m/s. This aligns with Wahid (2017) research, which states that wind speeds moving with the west monsoon are higher than those moving with the east monsoon. Higher wind speeds can help pollutants spread farther and cause more intense dilution of concentrations, thereby reducing concentrations (Yang et al., 2019).

#### 3.4 Potential Sources of Transboundary Emissions

##### 3.4.1 Air Masses Movement

The results of airflow analysis during the wet and dry season in non-rainfall period at altitudes of 15, 50, 100, and 200 magl are shown in Figure A1. In general,

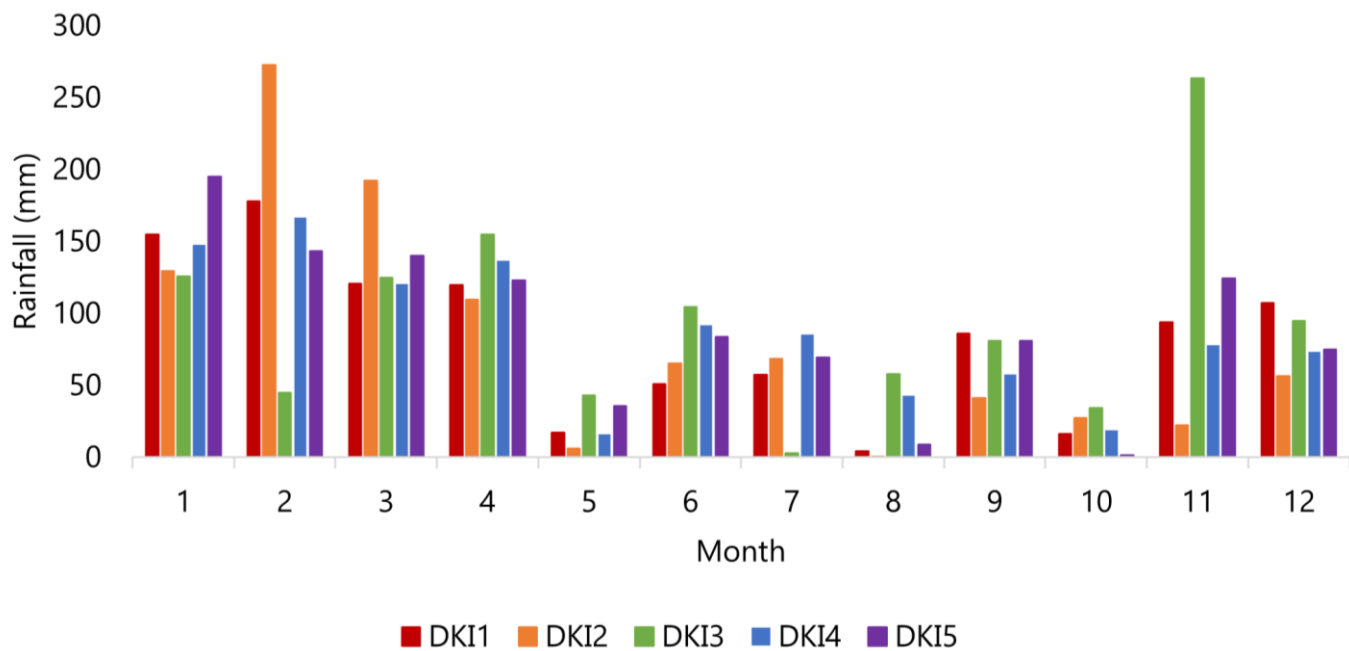


**Figure 2** Monthly rainfall characteristics during 2024 in all air quality monitoring stations

the wet season coincides with west monsoon while the dry season coincides with east monsoon (Ferijal et al., 2021). During the west monsoon, the airflow moving toward DKI1-DKI5 at altitudes of 15, 50, 100, and 200 magl has the same dominant direction across all layers. However, in January, the dominant wind direction is from the west-southwest, with a range of 63-99% (Table A2). These airflows pass through areas west of Jakarta, such as Tangerang and Tangerang City, in line with the southwest wind direction, for monitoring points DKI1, DKI2, DKI4, and DKI5. Meanwhile, for monitoring point DKI3, the airflow originates from Bogor and Depok districts, located south of monitoring point DKI3. In February, the dominant wind direction is from the west-northwest with a range of 51%-99% (Table A2). The airflow passes through areas west-northwest of Jakarta, such as Tangerang, Tangerang City, and South Tangerang, in line with the wind direction from the west-northwest, for monitoring points DKI1, DKI2, DKI3, and DKI5. Meanwhile, for the DKI4 monitoring point, the airflow originated from the Jakarta area, namely North Jakarta, Central Jakarta, and South Jakarta.

The similar pattern was observed during the east monsoon, where the airflow moving toward DKI1-DKI5 has the same dominant direction at altitudes of 15, 50, and 100 magl, but differs at the 200 magl layer (Figure A1). In July, the dominant wind direction was southeast-northeast with a range of 50%-70% (Table A2). This airflow passes through areas east of Jakarta, such as Bekasi and Bekasi City, in line with the southeast-northeast wind direction for monitoring points DKI1-DKI4. Meanwhile, for monitoring points DKI5, the air-

flow originates from the Jakarta area, specifically Central Jakarta, North Jakarta, and East Jakarta. In August, the dominant wind direction was southeast-northeast with a range of 52%-74% (Table A2). This airflow passes through areas east of Jakarta, such as Bekasi and Bekasi City, in line with the wind direction from the southeast and southeast-northeast for monitoring points DKI1-DKI5. In September, the dominant wind direction is from the northeast, ranging from 56% to 94% (Table A2). These air currents pass through areas east of Jakarta, such as Bekasi and Bekasi City, in line with the wind direction from the southeast-northeast, for monitoring points DKI1-DKI4. Meanwhile, for monitoring point DKI5, the air currents originate from the Jakarta area, specifically Central Jakarta and North Jakarta. Further, this highlights the

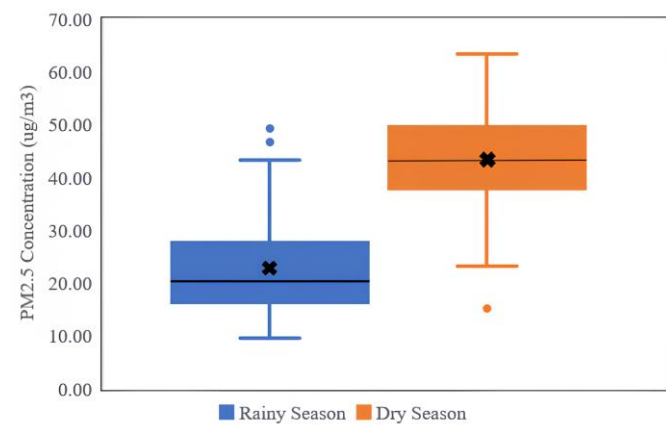


**Figure 3** PM2.5 concentration values in the DKI Jakarta in 2024 during non-rainfall periods ("x" refers to mean value and center line refers to median)

**Table 2** Summary of the polar plot showing local emission sources in DKI Jakarta during 2024

| Air Quality Monitoring Station | Dominant Wind       |                     | Wind Speed (m/s) |            | PM <sub>2.5</sub> ( $\mu\text{g}/\text{m}^3$ ) |            |
|--------------------------------|---------------------|---------------------|------------------|------------|--|------------|
|                                | Wet Season          | Dry Season          | Wet Season       | Dry Season | Wet Season                                     | Dry Season |
| DKI1                           | southwest           | northeast           | 0,5-2,5          | 0,5-1,5    | 10-20  | >50        |
| DKI2                           | southwest-northwest | northwest           | 0,5-1,5          | 0,5-1,5    | 20-40  | 40 - >50   |
| DKI3                           | southwest           | northwest-northeast | 0,5-2            | 0,5-2      | 10-20  | 40 - >50   |
| DKI4                           | northeast           | northeast           | 0,5-2,5          | 0,5-2,5    | 30-40  | 30 - >50   |
| DKI5                           | northwest           | northeast           | 0,5-5            | 0,5-4      | 1-20   | >50        |

effect of wind direction to air pollutant movement.

At an altitude of 200 magl during the dry season, atmospheric conditions are more stable and dry, resulting in a clearer boundary layer with inversion (Lan et al., 2024). At this altitude, there is no surface influence, so the Coriolis force and pressure gradient produce a different airflow pattern. This does not occur at an altitude of 200 mgl during the wet season because atmospheric conditions during the wet season are more unstable and humid with active convection causing stronger vertical mixing (Lan et al., 2024). This causes surface effects in the lower layer to spread vertically up to an altitude of 200 magl, so that the airflow patterns in the 15 magl, 50 magl, 100 magl, and 200 magl layers have the same dominant direction.

#### 3.4.2 Potential Sources of Interregional Emission

The movement of air currents during the west monsoon and east monsoon affects the movement of pollutants contained in these air currents. During the west monsoon, the dominant wind direction is nearly same at each altitude, so the pollutants contained within tend to spread (disperse) at altitudes of 15 magl to 200 magl, thereby affecting mixing and reducing concentrations. The distance pollutants are dispersed is determined by the speed of the airflow carrying them (Turyanti, 2011), which also affects the dilution of pollutant concentrations. Meanwhile, during the east monsoon, the airflow moving toward DKI1-DKI5 has the same dominant direction at the 15 magl, 50 magl, and 100 magl layers. As a result, pollutants transported by airflow tend to be restricted to the lower atmospheric layers, which can lead to elevated pollutant concentrations (Cruz et al., 2023). Meanwhile, in higher layers, air mass flow comes from different directions. Based on the analysis of air mass flow patterns and PM<sub>2.5</sub> concentrations in the areas it passes through, the potential emission sources contributing to air quality in Jakarta can be estimated.

The potential emission sources between DKI Jakarta regions during the wet season (west monsoon

period) and dry season (east monsoon period) at heights of 10 magl, 50 magl, 100 magl, and 200 magl are shown in Figure A2 and A3. The potential emission sources between DKI Jakarta regions during the wet season (west monsoon period) and dry season (east monsoon period) at heights of 10 magl, 50 magl, 100 magl, and 200 magl are shown in Figure A2 and A3. Meanwhile, a summary of emission sources between Jakarta regions based on the figures, including the percentage of dominant wind directions, estimated PM<sub>2.5</sub> contributions between regions, and areas with the potential to be emission sources in DKI1-DKI5, is shown in Table 6. The table shows that the dominant wind during the wet season (January) is from the southwest. Meanwhile, the dominant wind direction during the dry season (August), originates from the northeast. The percentage of dominant wind during the wet season is higher than during the dry season. This indicates that during the wet season, airflow movement in the 15 magl, 50 magl, 100 magl, and 200 magl atmospheric layers of Jakarta has more dominant airflow movement than during the dry season. This impacts the estimated PM<sub>2.5</sub> contribution between regions. The estimated contribution of PM<sub>2.5</sub> between regions in Jakarta during the wet season is lower than during the dry season. This occurs because, during the wet season, pollutants from emission sources in certain regions disperse and spread more quickly, resulting in a lower contribution of PM<sub>2.5</sub> from one region to another. Meanwhile, during the dry season, pollutants from emission sources in a particular region are dispersed over short distances with high pollutant concentrations, resulting in higher PM<sub>2.5</sub> contributions to other regions.

In the DKI5 region during the dry season, the estimated contribution of PM<sub>2.5</sub> from surrounding areas is more than 55  $\mu\text{g}/\text{m}^3$ . The high estimated contribution of PM<sub>2.5</sub> indicates that the emission sources in DKI5 during the 2024 dry season are dominated by surrounding areas, namely North Jakarta, Central Jakarta, and Bekasi. According to Pratama (2023), North Jakarta is home to the Priok and Muara Karang power

**Table 3** Potential sources of emission between regions in DKI Jakarta during 2024

| Air Quality Monitoring Station Locations | Percentage of Dominant Winds (%) |           | Estimated Contribution of PM <sub>2.5</sub> between Regions ( $\mu\text{g}/\text{m}^3$ ) |            | Potential Areas as Sources of Emissions           |  |
|--|----------------------------------|-----------|--|------------|---|--|
|  | Dry Season                       |           | Wet Season   | Dry Season | Wet Season  | Dry Season                                 |
|  | Southwest                        | Northeast |  |            |   |  |
| DKI1                                     | 63-99                            | 61-72     | 5-15   | 40-45      | West Jakarta, Tangerang City and Tangerang        | North Jakarta and Bekasi                   |
| DKI2                                     | 63-98                            | 58-74     | 5-15   | 40-55      | Central Jakarta, West Jakarta, and Tangerang City | Bekasi                                     |
| DKI3                                     | 68-99                            | 52-63     | 20-30  | 45-50      | Depok and Bogor Regency                           | Jakarta East, Bekasi City, and Depok       |
| DKI4                                     | 88-99                            | 53-72     | 35-40  | 30-45      | South Jakarta, South Tangerang, and Tangerang     | Bekasi City, and Bekasi                    |
| DKI5                                     | 63-89                            | 57-70     | 10-15  | >55        | Tangerang City and Tangerang                      | North Jakarta, Central Jakarta, and Bekasi |

plants, which are used to generate electricity for the DKI Jakarta and Banten regions. The Suralaya power plant is also suspected to be one of the causes of PM<sub>2.5</sub> in the Jakarta metropolitan area, as it uses coal as fuel. These power plants emit PM<sub>2.5</sub> concentrations into the atmosphere, which are then carried by air currents and measured by air quality monitoring stations in DKI5, resulting in high PM<sub>2.5</sub> concentrations in the DKI5 region.

Analysis of PM<sub>2.5</sub> emission sources in DKI Jakarta originating from interregional emission sources using HYSPLIT CWT shows the potential for significant cross-border emission sources, especially during the dry season or when the east monsoon winds occur. However, this study requires further development in terms of data validation. Data validation needs to be carried out comprehensively in each region through which air flows toward the study area. Nevertheless, it is hoped that this study can provide input for the government in formulating effective policies to manage and control air quality in Jakarta, particularly by installing instruments in locations where PM<sub>2.5</sub> has been identified.

#### 4. CONCLUSION

PM<sub>2.5</sub> concentrations during non-rainfall periods were substantially lower in the wet season (average 27.11  $\mu\text{g}/\text{m}^3$ ) than in the dry season (average 44.87  $\mu\text{g}/\text{m}^3$ ). Wind speeds during the west monsoon were generally higher than during the east monsoon,

reflecting the strong influence of seasonal monsoonal circulation. During the wet season (January–February), airflow predominantly originated from the southwest to northwest, whereas during the dry season (July–September) it shifted from the northeast to southeast. Airflow trajectories during the west monsoon were relatively linear and consistent across all analyzed heights (15–200 m above ground level), indicating uniform transport patterns within the lower troposphere. In contrast, during the east monsoon, curved airflow trajectories toward northern Jakarta were observed, particularly at higher altitudes, suggesting the influence of atmospheric stability and potential interregional emission sources.

Estimated interregional contributions to PM<sub>2.5</sub> concentrations ranged from 8–30  $\mu\text{g}/\text{m}^3$  during the wet season and increased substantially to 40–50  $\mu\text{g}/\text{m}^3$  during the dry season. Overall, the results demonstrate that PM<sub>2.5</sub> variability in Jakarta is strongly controlled by monsoonal wind speed, direction, and seasonal atmospheric stability, emphasizing the importance of considering vertical transport processes when assessing transboundary air pollution in the lower troposphere.

#### ACKNOWLEDGEMENT

We would like to express our deepest gratitude to Dinas Lingkungan Hidup DKI Jakarta for the permission and data provided. The assistance provided was crucial to the success of this research.

## REFERENCES

Almetwally, A.A., Bin-Jumah, M., Allam, A.A., 2020. Ambient air pollution and its influence on human health and welfare: an overview. *Environ Sci Pollut Res* 27, 24815–24830. <https://doi.org/10.1007/s11356-020-09042-2>

Beloconi, A., Vounatsou, P., 2021. Substantial Reduction in Particulate Matter Air Pollution across Europe during 2006–2019: A Spatiotemporal Modeling Analysis. *Environ. Sci. Technol.* 55, 15505–15518. <https://doi.org/10.1021/acs.est.1c03748>

Carslaw, D.C., Beavers, S.D., 2013. Characterising and understanding emission sources using bivariate polar plots and k-means clustering. *Environmental Modelling & Software* 40, 325–329. <https://doi.org/10.1016/j.envsoft.2012.09.005>

Choi, W., Ho, C.-H., Lee, Y., 2024. Temporal pattern classification of PM2.5 chemical compositions in Seoul, Korea using K-means clustering analysis. *Science of The Total Environment* 927, 172157. <https://doi.org/10.1016/j.scitotenv.2024.172157>

Cruz, M.T., Simpas, J.B., Sorooshian, A., Betito, G., Cambaliza, M.O.L., Collado, J.T., Eloranta, E.W., Holz, R., Topacio, X.G.V., Del Socorro, J., Bagtasa, G., 2023. Impacts of regional wind circulations on aerosol pollution and planetary boundary layer structure in Metro Manila, Philippines. *Atmospheric Environment* 293, 119455. <https://doi.org/10.1016/j.atmosenv.2022.119455>

Doherty, R.M., Heal, M.R., O'Connor, F.M., 2017. Climate change impacts on human health over Europe through its effect on air quality. *Environ Health* 16, 118. <https://doi.org/10.1186/s12940-017-0325-2>

Đorđević, D.S., Šolević, T.M., 2008. The contributions of high- and low altitude emission sources to the near ground concentrations of air pollutants. *Atmospheric Research* 87, 170–182. <https://doi.org/10.1016/j.atmosres.2007.08.005>

Ferijal, T., Batelaan, O., Shanafield, M., 2021. Spatial and temporal variation in rainy season droughts in the Indonesian Maritime Continent. *Journal of Hydrology* 603, 126999. <https://doi.org/10.1016/j.jhydrol.2021.126999>

Fujino, R., Miyamoto, Y., 2022. PM2.5 decrease with precipitation as revealed by single-point ground-based observation. *Atmospheric Science Letters* 23, e1088. <https://doi.org/10.1002/asl.1088>

Hao, Y., Liu, Y.-M., 2016. The influential factors of urban PM2.5 concentrations in China: a spatial econometric analysis. *Journal of Cleaner Production, Preventing Smog Crises* 112, 1443–1453. <https://doi.org/10.1016/j.jclepro.2015.05.005>

Hehua, Z., Qing, C., Shanyan, G., Qijun, W., Yuhong, Z., 2017. The impact of prenatal exposure to air pollution on childhood wheezing and asthma: A systematic review. *Environmental Research* 159, 519–530. <https://doi.org/10.1016/j.envres.2017.08.038>

Jiang, N., Zhu, C., Hu, Z.-Z., McPhaden, M.J., Chen, D., Liu, B., Ma, S., Yan, Y., Zhou, T., Qian, W., Luo, J., Yang, X., Liu, F., Zhu, Y., 2024. Enhanced risk of record-breaking regional temperatures during the 2023–24 El Niño. *Sci Rep* 14, 2521. <https://doi.org/10.1038/s41598-024-52846-2>

Kayes, I., Shahriar, S.A., Hasan, K., Akhter, M., Kabir, M.M., Salam, M., 2019. The relationships between meteorological parameters and air pollutants in an urban environment. *Global Journal of Environmental Science and Management* 5, 265–278. <https://doi.org/10.22034/gjesm.2019.03.01>

Khaniabadi, Y.O., Sicard, P., Takdastan, A., Hopke, P.K., Taiwo, A.M., Khaniabadi, F.O., De Marco, A., Daryanoosh, M., 2019. Mortality and morbidity due to ambient air pollution in Iran. *Clinical Epidemiology and Global Health* 7, 222–227. <https://doi.org/10.1016/j.cegh.2018.06.006>

Kravitz-Wirtz, N., Teixeira, S., Hajat, A., Woo, B., Crowder, K., Takeuchi, D., Kravitz-Wirtz, N., Teixeira, S., Hajat, A., Woo, B., Crowder, K., Takeuchi, D., 2018. Early-Life Air Pollution Exposure, Neighborhood Poverty, and Childhood Asthma in the United States, 1990–2014. *International Journal of Environmental Research and Public Health* 15. <https://doi.org/10.3390/ijerph15061114>

Lan, C.-W., Chen, C.-A., Lo, M.-H., 2024. The Role of Atmospheric Stabilities and Moisture Convergence in the Enhanced Dry Season Precipitation over Land from 1979 to 2021. *Journal of Climate* 37, 2881–2893. <https://doi.org/10.1175/JCLI-D-23-0287.1>

Li, Y., Tong, D.Q., Ngan, F., Cohen, M.D., Stein, A.F., Kondragunta, S., Zhang, X., Ichoku, C., Hyer, E.J., Kahn, R.A., 2020. Ensemble PM2.5 Forecasting During the 2018 Camp Fire Event Using the HYSPLIT Transport and Dispersion Model. *Journal of Geophysical Research: Atmospheres* 125, e2020JD032768. <https://doi.org/10.1029/2020JD032768>

Ma, Y., Wang, M., Wang, S., Wang, Y., Feng, L., Wu, K., 2020. Air pollutant emission characteristics and HYSPLIT model analysis during heating period in Shenyang, China. *Environmental Monitoring and Assessment* 193, 9. <https://doi.org/10.1007/s10661-020-08767-4>

Ma, Y., Zhao, H., Liu, Q., 2022. Characteristics of PM2.5 and PM10 pollution in the urban agglomeration of Central Liaoning. *Urban Climate* 43, 101170. <https://doi.org/10.1016/j.uclim.2022.101170>

Maheng, D., Bhattacharya, B., Zevenbergen, C., Pathirana, A., Maheng, D., Bhattacharya, B., Zevenbergen, C., Pathirana, A., 2023. Changing Urban Temperature and Rainfall Patterns in Jakarta: A Comprehensive Historical Analysis. *Sustainability* 16. <https://doi.org/10.3390/su16010350>

Manosalidis, I., Stavropoulou, E., Stavropoulos, A., Bezirtzoglou, E., 2020. Environmental and Health Impacts of Air Pollution: A Review. *Front. Public Health* 8. <https://doi.org/10.3389/fpubh.2020.00014>

Masiol, M., Vu, T.V., Beddows, D.C.S., Harrison, R.M., 2016. Source apportionment of wide range particle size spectra and black carbon collected at the airport of Venice (Italy). *Atmospheric Environment* 139, 56–74. <https://doi.org/10.1016/j.atmosenv.2016.05.018>

Ni, J., Zhao, Y., Li, B., Liu, J., Zhou, Y., Zhang, P., Shao, J., Chen, Y., Jin, J., He, C., 2023. Investigation of the impact mechanisms and patterns of meteorological factors on air quality and atmospheric pollutant concentrations during extreme weather events in Zhengzhou city, Henan Province. *Atmospheric Pollution Research* 14, 101932. <https://doi.org/10.1016/j.apr.2023.101932>

Pratama, R.A., 2023. Study Kelayakan LOLP (Loss Of Load Probability) pada PLTGU Unit Pembangkit Muara Karang. *Jurnal Teknologi Elektro* 14, 180–184. <https://doi.org/10.22441/jte.2023.v14i3.009>

Rawat, V., Singh, N., Singh, J., Rajput, A., Dhaka, S.K., Matsumi, Y., Nakayama, T., Hayashida, S., 2024. Assessing the high-resolution PM2.5 measurements over a Central Himalayan site: impact of mountain meteorology and episodic events. *Air Qual Atmos Health* 17, 51–70. <https://doi.org/10.1007/s11869-023-01429-7>

Sanguineti, P.B., Lanzaco, B.L., López, M.L., Achad, M., Palancar, G.G., Olcese, L.E., Toselli, B.M., 2020. PM2.5 monitoring during a 10-year period: relation between elemental concentration and meteorological conditions. *Environ Monit Assess* 192, 313. <https://doi.org/10.1007/s10661-020-08288-0>

Sharma, S., Sharma, R., Sahu, S.K., Kota, S.H., 2022. Transboundary sources dominated PM2.5 in Thimphu, Bhutan. *Int. J. Environ. Sci. Technol.* 19, 5649–5658. <https://doi.org/10.1007/s13762-021-03505-w>

Squizzato, S., Cazzaro, M., Innocente, E., Visin, F., Hopke, P.K., Rampazzo, G., 2017. Urban air quality in a mid-size city — PM2.5 composition, sources and identification of impact areas: From local to long range contributions. *Atmospheric Research* 186, 51–62. <https://doi.org/10.1016/j.atmosres.2016.11.011>

Suhery, N., Jaya, M.M., Khikmawati, L.T., Sarasati, W., Tanjov, Y.E., Larasati, R.F., Azis, M.A., Purwanto, A., Sari, I.P., Mainnah, M., Satyawan, N.M., 2023. Keterkaitan Musim Hujan dan Musim Angin dengan Musim Penangkapan Ikan Lemuru yang Berbasis di PPN Pengambangan. *Marine Fisheries: Journal of Marine Fisheries Technology and Management* 14, 77–90. <https://doi.org/10.29244/jmf.v14i1.44383>

Thangavel, P., Park, D., Lee, Y.-C., 2022. Recent Insights into Particulate Matter (PM2.5)-Mediated Toxicity in Humans: An Overview. *International Journal of Environmental Research and Public Health* 19, 7511. <https://doi.org/10.3390/ijerph19127511>

Turyanti, A., 2011. Analisis Pengaruh Faktor Meteorologi terhadap Konsentrasi PM10 Menggunakan Regresi Linier Berganda (Studi Kasus: Daerah Dago Pakar dan Cisaranten, Bandung). *Agromet* 25, 29–36. <https://doi.org/10.29244/j.agromet.25.1.29-36>

Wahid, M.A., 2017. Mengidentifikasi Besar Kecepatan Angin dan Energinya Melalui Data Ncep/Ncar Reanalysis dan 5 Stasiun Bmkg di Provinsi Aceh. *Phi: Jurnal Pendidikan Fisika dan Terapan* 3, 1–10. <https://doi.org/10.22373/p-jpft.v3i1.7445>

Wu, W., Zha, Y., Zhang, J., Gao, J., He, J., 2014. A temperature inversion-induced air pollution process as analyzed from Mie LiDAR data. *Science of The Total Environment* 479–480, 102–108. <https://doi.org/10.1016/j.scitotenv.2014.01.112>

Yang, Q., Yuan, Q., Li, T., Shen, H., Zhang, L., Yang, Q., Yuan, Q., Li, T., Shen, H., Zhang, L., 2017. The Relationships between PM2.5 and Meteorological Factors in China: Seasonal and Regional Variations. *International Journal of Environmental Research and Public Health* 14. <https://doi.org/10.3390/ijerph14121510>

Yin, X., Kang, S., Rupakheti, M., de Foy, B., Li, P., Yang, J., Wu, K., Zhang, Q., Rupakheti, D., 2021. Influence of transboundary air pollution on air quality in southwestern China. *Geoscience Frontiers* 12, 101239. <https://doi.org/10.1016/j.gsf.2021.101239>

Zhang, B., Jiao, L., Xu, G., Zhao, S., Tang, X., Zhou, Y., Gong, C., 2018. Influences of wind and precipitation on different-sized particulate matter concentrations (PM2.5, PM10, PM2.5–10). *Meteorol Atmos Phys* 130, 383–392. <https://doi.org/10.1007/s00703-017-0526-9>

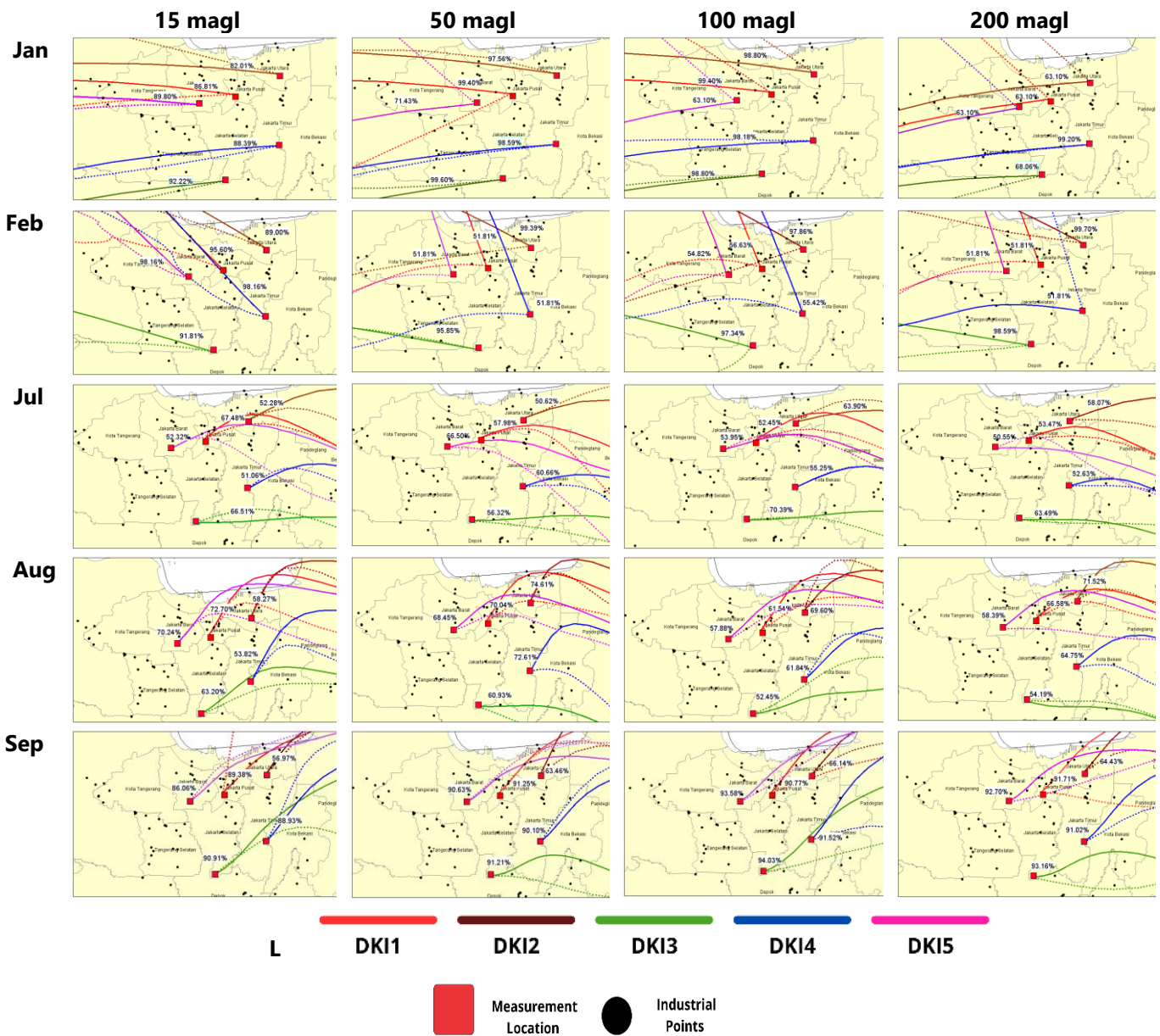
## ANNEX

**Table A1** Non-rainfall periods data for DKI Jakarta in 2024

| <b>Location/Station Name</b>      | <b>January</b> | <b>February</b> | <b>July</b> | <b>August</b> | <b>September</b> |
|-----------------------------------|----------------|-----------------|-------------|---------------|------------------|
| DKI1/ Bundaran HI-Central Jakarta | 22-26          | 17-21           | 9-31        | 3-31          | 15-30            |
| DKI2/ Kelapa Gading-North Jakarta | 22-26          | 18-24           | 1-31        | 1-31          | 1-30             |
| DKI3/ Jagakarsa-South Jakarta     | 8-30           | 1-20            | 1-31        | 1-31          | 15-30            |
| DKI4/ Lubang Buaya-East Jakarta   | 8-26           | 15-21           | 9-31        | 1-31          | 15-30            |
| DKI5 / Kebon Jeruk-West Jakarta   | 22-26          | 15-21           | 9-31        | 1-31          | 15-30            |

**Table A2** Summary of airflow during the west monsoon and east monsoon in DKI Jakarta during 2024

| <b>Month</b> | <b>Percentage of Dominant Winds</b> | <b>Dominant Wind Direction</b> |
|--------------|-------------------------------------|--------------------------------|
| January      | 63-99%                              | west-southwest                 |
| February     | 51-99%                              | west-northwest                 |
| July         | 50-70%                              | southeast-northeast            |
| August       | 52-74%                              | southeast-northeast            |
| September    | 56-94%                              | northeast                      |



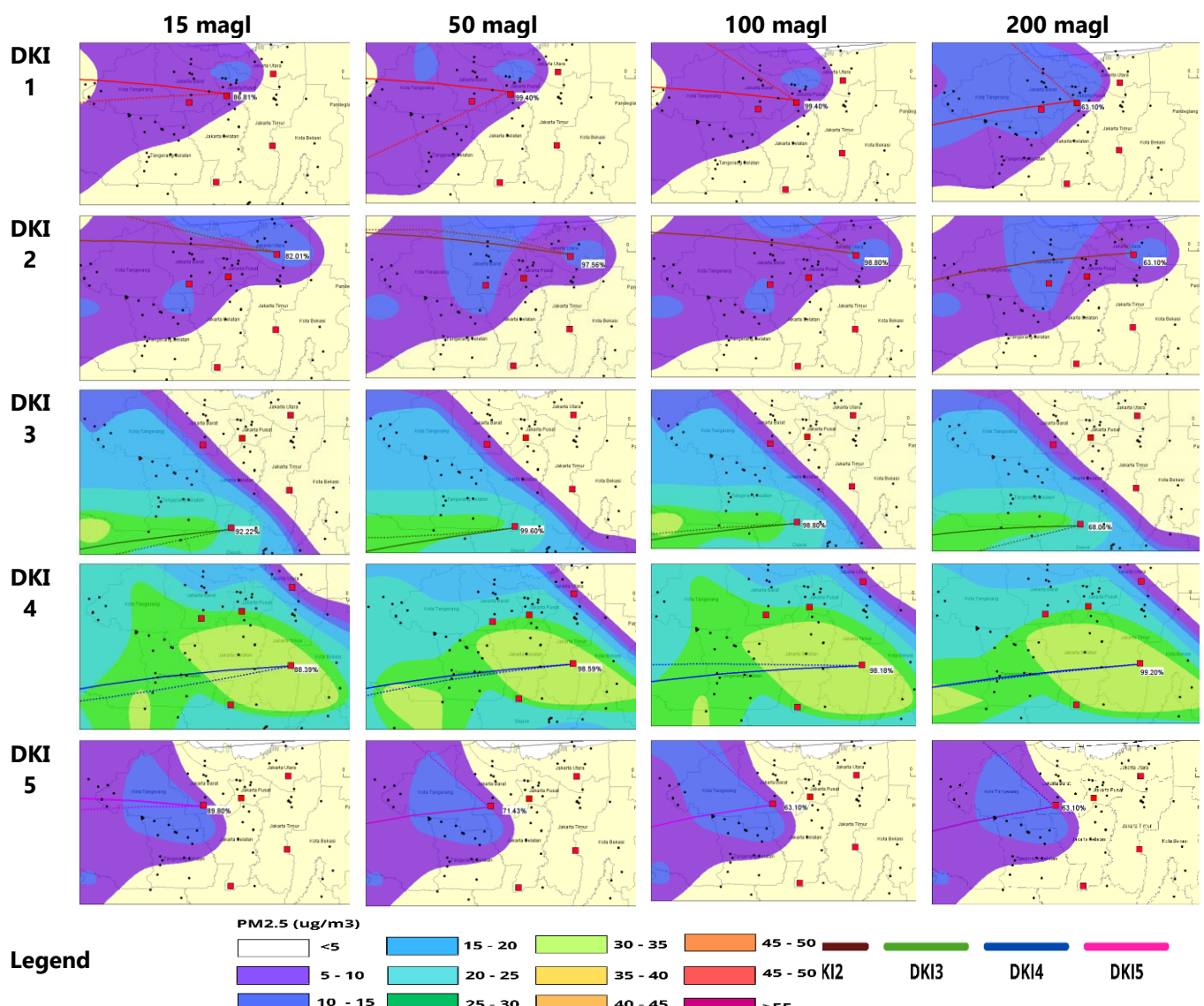


**Figure A2** Estimated contribution of PM2.5 emission sources in the DKI Jakarta in January 2024 during 372 non-rainfall periods (HYSPLIT model output). mgl refers to meters above ground level

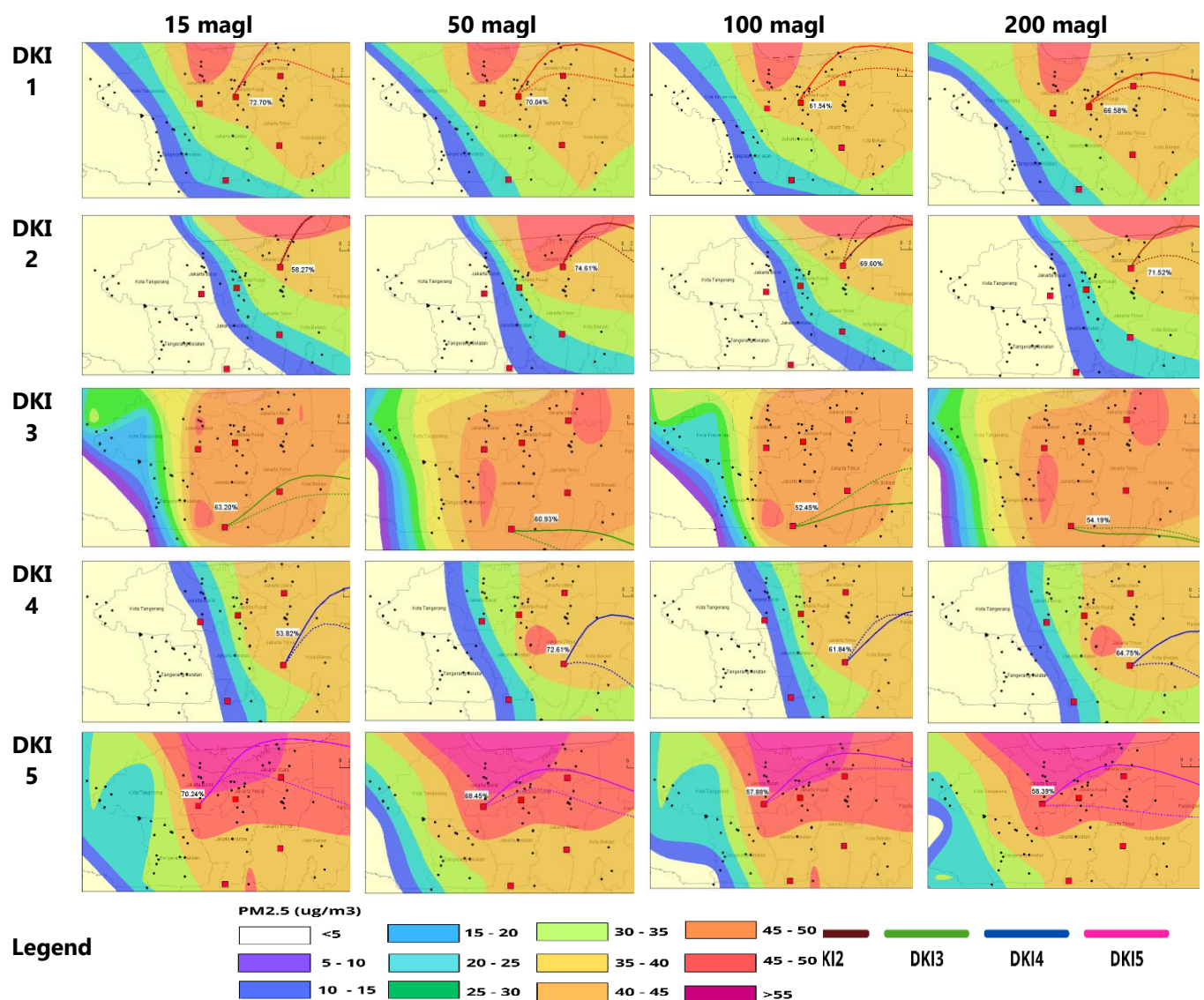


**Figure A3** Estimated contribution of PM2.5 emission sources in the DKI Jakarta in August 2024 during 372 non-rainfall periods (HYSPLIT model output), magl refers to meters above ground level